Japanese Journal of Applied Physics **59**, SBBC03(1-5) (2020)
DOI:10.7567/1347-4065/ab4b1e

Atomic Diffusion Bonding Using Oxide Underlayers for Optical Applications

G. Yonezawa[1,4]*, Y. Takahashi[2], Y. Sato[1], S. Abe[3], M. Uomoto[4] and T. Shimatsu[4,5]*

1 Sony Corp., 1-7-1 Konan Minato-ku, Tokyo, 108-0075, Japan
2 Sony Imaging Products & Solutions Inc., 1-7-1 Konan Minato-ku, Tokyo, 108-0075, Japan
3 Sony Global Manufacturing & Operations Corporation, 1-7-1 Konan Minato-ku, Tokyo, 108-0075, Japan
4 Frontier Research Institute for Interdisciplinary Sciences (FRIS), Tohoku University, Sendai 980-8578, Japan
5 Research Institute of Electrical Communication (RIEC), Tohoku University, Sendai 980-8577, Japan

*E-mail: gen.yonezawa@sony.com; shimatsu@riec.tohoku.ac.jp

Atomic diffusion bonding (ADB) of quartz glass wafers using thin Ti films, with SiO_2 underlayers on wafer surfaces, provides 100% light transmittance at the bonded interface along with strong bonding energy, after post-bonded low-temperature annealing. Cross-section images obtained using transmission electron microscopy (TEM) show that the bonded interface after annealing at 350°C consists of amorphous structure including nanocrystalline grains. Structural analysis using electron energy loss spectroscopy (EELS) shows that post-bonded annealing enhances oxidation of Ti with oxygen dissociated from SiO_2 underlayers, and that Ti oxides form close to TiO_2 or Ti_4O_7. This oxidation provides 100% light transmittance with high bonding strength attributable to the annealing. Moreover, we applied this technique for bonding glass and sapphire wafers using SiO_2-Nb_2O_5 underlayers, demonstrating that 100% light transmittance and control of refractive index matching are achieved simultaneously at the bonded interface.

1. Introduction

In recent years, the power and wall-plug efficiency performance of blue laser diodes have improved.[1)] Consequently, high-brightness liquid crystal on silicon (LCOS) projector products equipped with laser light sources are used[2)] increasingly for digital cinema, projection mapping, and simulation. Such LCOS systems usually use a polarizing beam splitter (PBS) for RGB channels.[3)] The PBS transmits p-polarized light and reflects s-polarized light. However, as the projector's brightness increases,[4-6)] the optical density inside the optical element also increases such that the organic adhesive in the optical interface becomes less reliable because of the strong photon and thermal energy of blue light emitted from the laser diode. New inorganic bonding methods that provide both high light transmittance and high bonding strength are necessary for optical interfaces of high optical density devices. In addition, bonding interface is also required to meet optical index matching at the bonded interface to avoid Fresnel's loss[7)] like that optical adhesive with refractive index matching to substrate is selected.[8-10)]

Atomic diffusion bonding (ADB) of two flat wafers with thin metal films is a promising process to achieve room-temperature wafer bonding[11–15)] along with surface-activated bonding.[16–19)] Actually, ADB can be done even with film thickness of a few angstroms on each side. Thin Ti films are useful to achieve high light transmittance while maintaining high bonding strength to bond oxide wafers such as synthetic quartz crystal[14, 15)]. However, optical energy absorption of 2% remains at the bonded interface, even when the wafers are bonded using 0.2 nm thick Ti films on each side.

To resolve this difficulty, we propose ADB using oxide underlayers to provide 100% light transmittance at the bonded interface.[20)] Here, 100% light transmittance means that loss of optical power at the bonded interface is lower than a detection limit. Figure 1 provides the process scheme of atomic diffusion bonding with oxide underlayers and post-bonded annealing process. For this process, oxide underlayers were deposited on wafers. Then the wafers with oxide underlayers were bonded using thin metal film in vacuum at room temperature as a usual atomic diffusion process. Thereafter, the bonded sample was taken out from the vacuum chamber, and was annealed in air. As a primitive study, we deposited SiO_2 underlayers on quartz glass wafers using ion-beam assisted deposition (IAD). The wafers with SiO_2 underlayers were bonded using thin Ti films in vacuum at room temperature as a usual atomic diffusion process. After post-annealing at 300 °C, 100% light transmittance at the bonded interface was achieved, even for the interface bonded using 1-nm-thick Ti film on each side, along with surface free energy for the bonded interface greater than 2 J/m^2.[20)] Cross-section images observed using transmission electron microscopy (TEM) revealed that the bonded interface after annealing was much thicker than the as-bonded interface and that it was more than twice the original total thickness of Ti films.[21)] This finding suggests that SiO_2 underlayers enhance Ti oxide formation with oxygen dissociated from SiO_2 underlayers by annealing, providing high 100% light transmittance with high bonding strength. It is reasonable to infer that oxide materials other than SiO_2 are useful for the underlayer. Using adequate oxide materials other than SiO_2 for underlayers can enable tuning of the optical refractive index at the bonded interface between optical wafers with any optical refractive index: not just that of quartz glass wafers. Such materials would extend the application of this bonding technique to almost all optical interfaces between mirror-polished surfaces of any material.

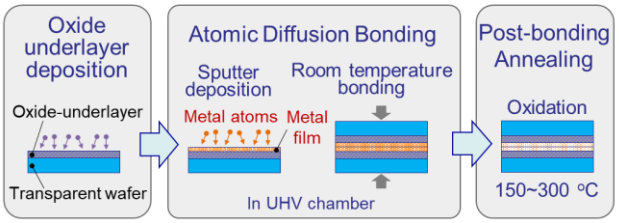

Fig. 1. Schematic illustration of atomic diffusion bonding with oxide underlayers and post-bonded annealing.

This study elucidated the interface nanostructure of SiO_2 films bonded with thin Ti films to clarify the mechanism providing 100% light transmittance at the bonded interface using electron energy loss spectroscopy (EELS).[22] Moreover, to confirm the potential of this bonding technique for use with various optical interfaces, we examined the ADB of glass and sapphire wafers using SiO_2-Nb_2O_5 composite underlayers that provide both refractive index matching and high light transmittance at the bonded interface.

2. Experimental methods

In atomic diffusion bonding, wafers with oxide underlayers were introduced into a vacuum chamber with base pressure of less than 5×10^{-7} Pa. Thin Ti films were fabricated using sputter deposition on the oxide underlayer surfaces of both sides of wafers. Subsequently, the two Ti films on the wafers were bonded under vacuum at room temperature. For this study, Ti was used because of its high light-transmittance characteristics over a wide range of the spectrum, a large self-diffusion coefficient, and high film adhesion strength on wafers. The Ti film thickness on each side was defined as δ. In post-bonded annealing processes, the bonded wafers were removed from the vacuum chamber into the atmosphere and were heated in air using an oven. The annealing temperature was varied from room temperature to 400°C. The annealing time was fixed at 1 hr.

In an earlier part of this study, quartz glass wafers with SiO_2 underlayers were bonded using ADB with thin Ti films (δ=1 nm) and were used for EELS analysis. The sample structure is presented schematically in Fig. 2(A).

In the latter section of this paper, as shown in Fig. 2(B), we used underlayers of a composite material: SiO_2-Nb_2O_5, which is commonly used industrially for optical thin films.

The Optical refractive index measured using the Fraunhofer helium d-spectral line with 587.6 nm wavelength, which is often used for lens materials, was used in this study. It was defined as n_d. The value of n_d for SiO_2 ($n_d(SiO_2)$) is 1.46. That for Nb_2O_5 ($n_d(Nb_2O_5)$) is 2.35. The value of n_d for SiO_2-Nb_2O_5 composite materials can be controlled by adjusting the relative volume fraction of SiO_2 and Nb_2O_5.[23, 24] As seen in Table I, two bonded samples were fabricated as sample A and sample B. The former comprises glass substrates (Eagle XG; Corning Inc.) with n_d=1.52 bonded using SiO_2-Nb_2O_5 composite underlayers with n_d=1.52 (tuned to be identical to that of the glass substrate). The latter is a sapphire substrate with n_d=1.76 bonded using SiO_2-Nb_2O_5 composite underlayers with n_d=1.77 (almost identical to that of a sapphire substrate).

Two-inch-diameter micro-polished wafers (synthetic quartz glass, glass, or sapphire) with 0.5 mm thickness were used as substrates. SiO_2 underlayers of 5000-nm film thickness were deposited using ion-beam assisted deposition (IAD). After SiO_2 underlayer deposition, the SiO_2 underlayer surface was finely micro-polished using chemical mechanical polishing (CMP). After the CMP process, the surface roughness S_a evaluated using atomic force microscopy (AFM) was 0.3 nm or less. Radical-assisted sputtering (RAS)[24–27] was used to deposit 5000-nm-thick SiO_2-Nb_2O_5 film underlayers on the wafer surface. Actually, RAS method is often used for the deposition of manufacturing optical filter parts for digital cameras and LCD projectors. The oxide underlayer surface was finely micro-polished using CMP. The value of S_a after the CMP process was 0.5 nm or less.

The light-transmittance spectrum of the sample was measured using an optical spectrometer. Fresnel loss between the wafer surfaces and air was excluded using the following equation (1).

$$T = (1 - R1)t(1 - R2),\ t = \frac{T}{(1-R1)(1-R2)} \qquad (1)$$

Here, T signifies total transmittance, $R1$ expresses the incident-side surface reflectance, $R2$ denotes the exit-side reflectance, and t stands for the bonded interface transmittance. Surface free energy at the bonded interface, γ, was assessed using the blade method reported by Maszara.[28]

3. Results and discussion

3.1 Bonded interface nanostructure providing 100% light transmittance

Quartz glass wafers with SiO_2 underlayers were bonded using ADB with Ti films (δ=1 nm) and were used for TEM and EELS analyses. As described in an earlier paper[20], light transmittance of 100% was achieved at post-bonded annealing temperature of 300°C even with δ of 1.0 nm. Moreover, post-bonded annealing enhanced the γ values of wafers. Actually, we were unable to evaluate γ value after the annealing at 300°C because the blade could not be inserted between the wafers.

Figure 3 presents TEM cross-section images of the bonded interface for (A) an as-bonded sample and (B) after annealing at 350°C. The thickness of the bonded interface after annealing was 4.4 nm, which was much thicker than that of as-bonded interface. This thickness is more than

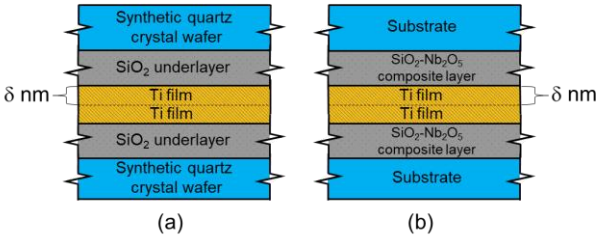

Fig. 2. Sample structures used for the study.

Table I. Optical substrates of two types bonded using SiO_2-Nb_2O_5 composite underlayers, sample A and sample B. Materials of substrates, the values of n_d of substrates and SiO_2-Nb_2O_5 underlayers are shown.

		Sample A	Sample B
Substrate	Material	Glass (Eagle XG, Corning)	Sapphire
	n_d	1.52	1.76
n_d of SiO_2-Nb_2O_5 composite underlayers		1.52	1.77

twice that of the original total thickness of Ti films. Crystal lattice images of several quantities of lattices with random orientation were partially observed in image (B) but no electron diffraction patterns were observed. This result suggested that the thick bonded interface consisted of an amorphous structure including nanocrystalline grains. The increase of interface thickness by annealing is likely to be attributable to the enhancement of Ti oxidation with oxygen dissociated from SiO_2 underlayers. However, the interface between Ti films and SiO_2 underlayers was clear even after the annealing, indicating that the diffusion of Ti to SiO_2 underlayers is negligible even after annealing at 350°C.

The center of the bonded interface thickness was analyzed using EELS. Figure 4(A) presents EELS spectra of these samples. Spectra around Ti-L edge with high magnification are portrayed in Fig. 4(B). Two peaks of Ti-L edge and weak peaks of O-K edge were observed in the as-bonded sample. These peaks suggest that the as-bonded interface consists of slightly oxidized Ti or Ti-O.[29–31] After annealing, peaks of O-K edge were clearly observed. Two peaks of Ti-L edge shifted to the high energy side. Moreover, a weak peak corresponding to the peak positions of crystalline TiO_2 or Ti_4O_7 [29–31] appeared on the left side shoulder of Ti-L_3 by annealing. These results suggest that annealing enhanced oxidation of Ti and that Ti oxides close to TiO_2 or Ti_4O_7 were formed in the bonded interface. Figure. 5(A) presents an image of the bonded interface after 350°C annealing observed using bright field scanning transmission electron microscopy (BF-STEM). The EELS spectra at points A, B (center), and C are shown in (B).

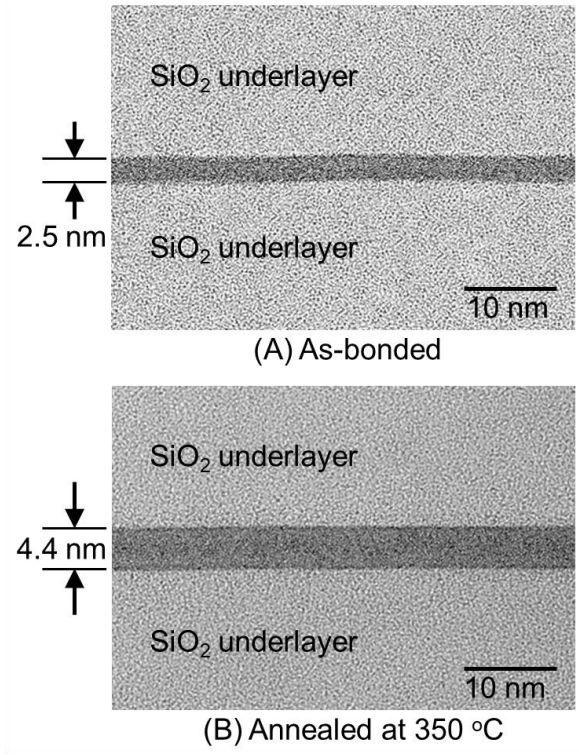

Fig. 3. TEM cross-section images of the bonded interface: (A) as-bonded sample and (B) after annealing at 350°C. SiO_2 films on quartz glass wafers were bonded using ADB with Ti(1.0 nm) on each side.

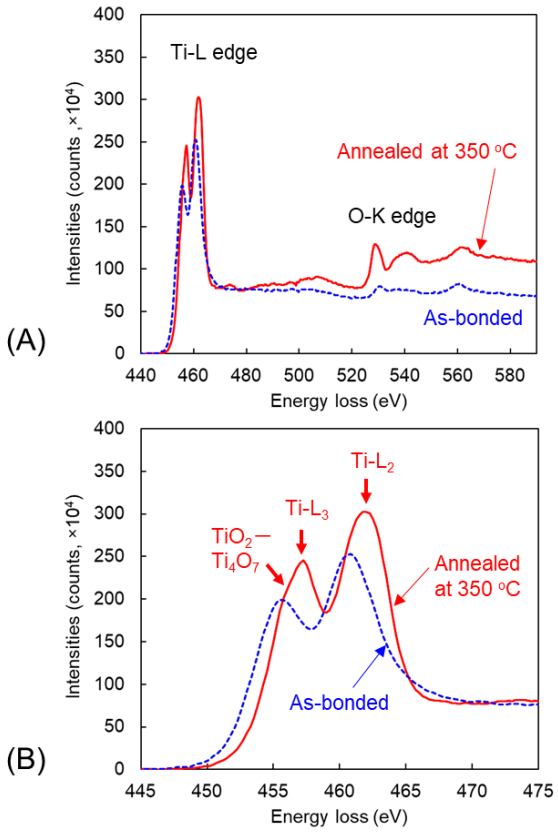

Fig. 4. (A) EELS Spectra at the center of the bonded interface thickness for samples shown in Fig. 3. (B) Spectra around Ti-L edge with high magnification.

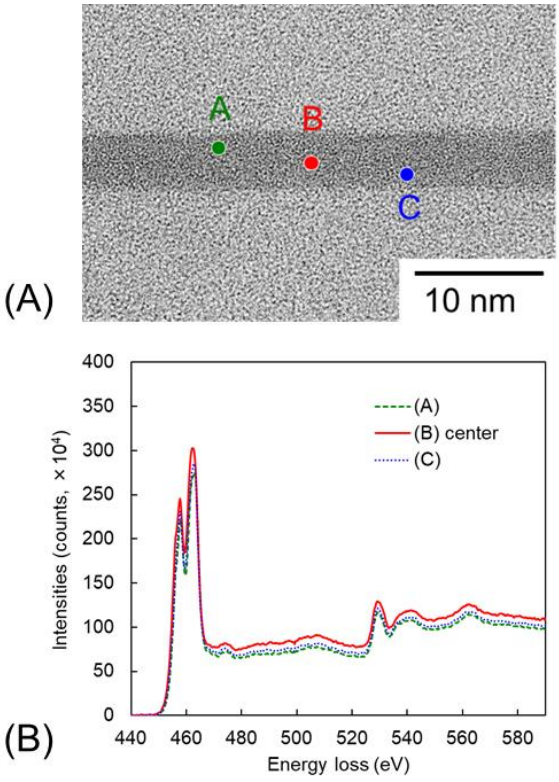

Fig. 5. (A) Image of the bonded interface after 350°C annealing observed using bright field scanning transmission electron microscopy (BF-STEM). (B) EELS spectra at points A, B(center), and C in (A).

Three spectra are mutually overlapped, indicating high uniformity of Ti oxide formation in the bonded interface. The diffusion length of oxygen dissociated from SiO_2 underlayers is likely to be much larger than the Ti thickness, although diffusion of Ti to SiO_2 underlayers is negligible, which results in the homogeneous formation of Ti oxide with sharp boundaries.

Here, ADB for these samples was performed using 1 nm thick Ti film on each side. Assuming that total 2 nm thick Ti films form oxide compounds with oxygen dissociated from SiO_2 underlayers, then a simple calculation revealed that the thicknesses of the formed oxide materials are 3.5 nm for TiO_2 (rutile) and 4.7 nm for Ti_4O_7. These thicknesses show good agreement with those observed in TEM images in Fig. 3. This agreement supports our inference that the interface structure after the 350°C annealing is Ti oxides close to TiO_2 or Ti_4O_7.

These structural analyses indicated that oxygen dissociated from oxide layers enhanced Ti film oxidation, providing high 100% light transmittance with high bonding strength attributable to the annealing.

3.2 High transmittance bonding with optical refractive matching

Figure 6 presents the values of the light transmittance at 587.6 nm wavelength for glass wafers (n_d=1.52) with SiO_2-Nb_2O_5 underlayers (n_d=1.52) bonded using Ti films (δ=1 nm) as a function of annealing temperature (solid line). The 587.6 nm wavelength is identical to that used for the definition of n_d. Results for synthetic quartz glass wafers using SiO_2 underlayers bonded with identically thick Ti films[20] are also shown for comparison (dotted line). The light transmittance for glass wafers with SiO_2-Nb_2O_5 underlayers increased gradually, achieving 100% at the annealing temperature of 300°C. The variation as a function of annealing temperature is almost identical to that of synthetic quartz glass wafers using SiO_2 underlayers, indicating that the oxidation of Ti films with oxygen dissociated from SiO_2-Nb_2O_5 underlayers was controlled identically to that from SiO_2 underlayers, although the film deposition techniques used for these films differed. Moreover, achievement of 100% light transmittance at the bonded interface indicated good refractive index matching using SiO_2-Nb_2O_5 underlayers. Actually, average light transmittance of 400–700 nm was also 100% achieved in this sample.

Figure 7 presents light transmittance values at the 587.6 nm wavelength for sapphire wafers (n_d=1.76) with SiO_2-Nb_2O_5 underlayers (n_d=1.77) bonded using Ti films (δ=0.5 nm) as a function of the annealing temperature (solid line). Results for synthetic quartz glass wafers using SiO_2 underlayers bonded with identically thick Ti films[20] are also shown for comparison (dotted line). The light transmittance for as-bonded sapphire wafers with SiO_2-Nb_2O_5 underlayers was higher than that with synthetic quartz glass wafers using SiO_2 underlayers. This higher transmittance is attributable mainly to the difference of film deposition method of underlayers. The light transmittance for as-bonded sapphire wafers with SiO_2-Nb_2O_5 underlayers increased further as the annealing temperature increased and achieved 99% at annealing temperature of 400°C. It is noteworthy that the light transmittance did not achieve 100%, even at 400°C, because of a slight difference of refractive index matching between sapphire wafers (n_d=1.76) with SiO_2-Nb_2O_5 underlayers (n_d=1.77).

4. Conclusions

Results indicate that post-bonded annealing at 350°C enhances oxidation of Ti films with oxygen dissociated from SiO_2 underlayers, and indicate that Ti oxides close to TiO_2 or Ti_4O_7 are formed in the interface. These phenomena provide 100% light transmittance with high bonding strength attributable to the annealing. Moreover, our application of this bonding technique for glass and sapphire wafers using SiO_2-Nb_2O_5 underlayers demonstrated that 100% light transmittance and control of refractive index matching were achieved simultaneously at the interface bonded using thin Ti films.

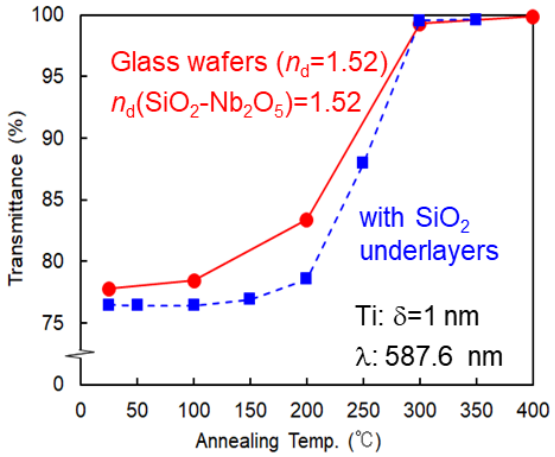

Fig. 6. Values of the light transmittance at 587.6 nm wavelength for glass wafers (n_d=1.52) with SiO_2-Nb_2O_5 underlayers (n_d=1.52) bonded using Ti films (δ=1 nm) as a function of annealing temperature (solid line). Results for synthetic quartz glass wafers using SiO_2 underlayers bonded with identically thick Ti films[20] are also shown for comparison (dotted line).

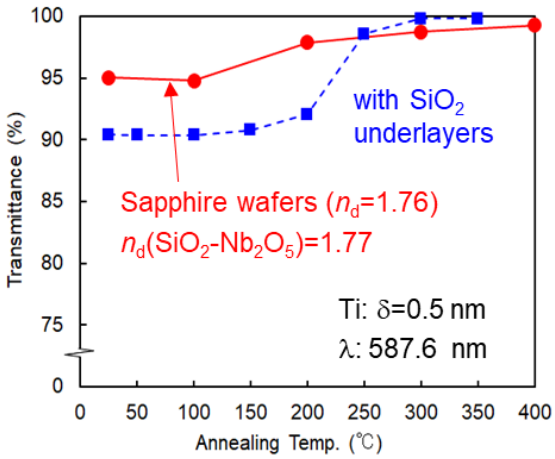

Fig. 7. Values of light transmittance at 587.6 nm wavelength for sapphire wafers (n_d=1.76) with SiO_2-Nb_2O_5 underlayers (n_d=1.77) bonded using Ti films (δ=0.5 nm) as a function of the annealing temperature (solid line). Results for synthetic quartz glass wafers using SiO_2 underlayers bonded with identically thick Ti films[20] are also shown for comparison (dotted line).

As described in our earlier paper,[20] the necessary annealing temperature for 100% light transmittance can be reduced to 150°C using suitable deposition techniques. It is reasonable to infer that oxide materials other than SiO_2 and SiO_2-Nb_2O_5 are useful for the underlayer. ADB using oxide underlayers, which is applicable to almost all optical interfaces between mirror-polished surfaces of any material, is expected to be useful to fabricate optical devices with high optical density such as high-brightness projectors with laser light sources. Moreover, one can reasonably infer that achievement of 100% light transmittance at the bonded interface by oxidation enhancement indicates a lack of electrical conductivity at the bonded interface, and that this method is applicable for fabricating new electronic devices.

References

1) Yoshitaka Nakatsu, Yoji Nagao, Kazuma Kozuru, Tsuyoshi Hirao, Eiichiro Okahisa, Shingo Masui, Tomoya Yanamoto, and Shin-ichi Nagahama, Proc. SPIE **10918,** Gallium Nitride Materials and Devices XIV, 109181D (2019).
2) Matthew S. Brennesholtz, SID Symposium Digest of Technical Papers **48** [1], 510 (2017).
3) M. Robinson, J. Chen, and G. D. Sharp, Journal of The Society for Information Display **14** [3], 303 (2006).
4) Hiroki Morita, Yuki Maeda, Izushi Kobayashi, Yoshihisa Sato, Tsuneharu Nomura, and Hiroki Kikuchi, SID Symposium Digest of Technical Papers **48** [1], 517 (2017).
5) Yoshikazu Komatsu, Yoshiki Kashihara, Jun Nishikawa, Ryo Yoshida, Tsuneharu Nomura, and Koichiro Ishii, SID Symposium Digest of Technical Papers **45** [1], 900 (2014).
6) Yuki Maeda, Yutaka Imai, Masahiro Ishige, Izushi Kobayashi, Kojiro Murakami, Takahiro Mochizuki, Tsuneharu Nomura, and Hiroki Kikuchi, SID Symposium Digest of Technical Papers **46** [1], 362 (2014).
7) Max Born, and Emil Wolf, Principles of Optics, (7th expanded ed.) Cambridge University Press, 65 (1999).
8) Krithika S. Prabhu, Tony L. Schmitz, Peter G. Ifju, and John G. Daly, Proc. SPIE **6665**, New Developments in Optomechanics, 666507 (2007).
9) David S. Stone, and Samantha R. Connor, Proc. SPIE **3937**, Micro- and Nano-photonic Materials and Devices, 144 (2000).
10) A. Priyadarshi, L. Shimin, S. G. Mhaisalkar, R. Rajoo, E. H. Wong, V. Kripesh, and E. B. Namdas, Journal of Applied Polymer Science **98** [3], 950 (2005).
11) T. Shimatsu, R. H. Mollema, D. Monsma, E. G. Keim and J. C. Lodder, J. Vac. Sci. Technol. A **16**, 2125 (1998).
12) T. Shimatsu and M. Uomoto, J. Vac. Sci. Technol., B **28**, 706 (2010).
13) T. Shimatsu, and M. Uomoto, ECS Transactions **33** [4], 61 (2010).
14) T. Shimatsu, and M. Uomoto, ECS Transactions **64** [5], 317 (2014).
15) M. Ichikawa, S. Endo, H Sagawa, A. Fujioka, T. Kosugi, T. Mukai, M. Uomoto, and T. Shimatsu, ECS Trans. **75** [9], 53 (2016).
16) T. Suga, K. Miyazawa, and Y. Yamagata, MRS Internal Meeting on Advanced Materials, Materials Research Society **8**, 257 (1989).
17) T. Suga, Y. Takahashi, H. Takagi, B. Gibbesch, and G. Elssner, Acta Metall. Mater. **40**, s133 (1992).
18) F. S. Ohuchi and T. Suga, Transactions of the Material Research Society of Japan **16B**, 1195 (1994).
19) Jun Utsumi, Kensuke Ide, and Yuko Ichiyanagi, Japanese Journal of Applied Physics **55** [2], 026503 (2016).
20) G. Yonezawa, Y. Takahashi, Y. Sato, S. Abe, M. Uomoto, and T. Shimatsu, ECS Transactions **86** [5], 233 (2018).
21) G. Yonezawa, Y. Takahashi, Y. Sato, S. Abe, M. Uomoto, and T. Shimatsu, Proc. 6th Int. Workshop Low Temperature Bonding for 3D Integration, 63 (2019) [DOI: 10.23919/LTB-3D.2019.8735120]
22) Ray Egerton, Physics World **10 [**4], 47 (1996).
23) M. Cevro, Thin Solid Films, **258** [1-2], 91 (1995).
24) Yousong Jiang, Yizhou Song, Takesi Sakurai, Ming Li, and Haiqian Wang, Journal of Advanced Science **16** [1], 1 (2004).
25) H. A. Macleod: Thin-Film Optical Filters, ed. WT Welford, (Imperial College, London), Third ed. Institute of Physics Publishing, 588 (2000).
26) Ekishu Nagae, Takeshi Sakurai, and Shigeharu Matsumoto, in Optical Interference Coatings, OSA Technical Digest Series (Optical Society of America), 588 (2001).
27) Yousong Jiang, Ming Li, Haiqian Wang, and Jeff Hou, In Optical Interference Coatings, paper ME4 (2004).
28) M. P. Maszara, G. Goetz, A. Cavigila, and J. B. McKitterick, J. Appl. Phys. **64**, 4943 (1988).
29) E. Stoyanov, F. Langenhorst, and G. Steinle-Neumann, American Mineralogist **92**, 577 (2007).
30) Lottiaux, M., Boulesteix, C., Nihoul, G., Varnier, F., Flory, F., Galindo, R., and Pelletier, E., Thin Solid Films **170 [**1], 107 (1989).
31) Brydson, R., Williams, B. G., Engel, W., Sauer, H., Zeitler, E., and Thomas, J. M., Solid State Communications **64** [4], 609 (1987).